MODAL ACOUSTIC EMISSION OF DAMAGE ACCUMMULATION IN WOVEN SiC/SiC AT ELEVATED TEMPERATURES

Gregory N. Morscher
Resident Research Associate (Case Western Reserve University)
NASA Lewis Research Center
MS 106-5
Cleveland, Ohio 44135

Ceramic matrix composites exhibit significant nonlinear stress-strain behavior that makes them attractive as potential materials for many high temperature applications. The mechanisms for this nonlinear stress-strain behavior are all associated with various types of damage in the composites, e.g. transverse matrix cracks and individual fiber failures. Modal acoustic emission has been employed to aid in discerning the damage accumulation that occurs during elevated temperature tensile stress-rupture of woven Hi-Nicalon™ fiber, BN interphase, SiC matrix composites. It is shown that modal acoustic emission is an effective monitor of the relative damage accumulation in the composites and locator of the damage and failure events as a function of strain (stress), time at temperature, and temperature gradients along the length of the elevated temperature test specimen.

INTRODUCTION

Traditional* acoustic emission (AE) has been used to monitor the damage which occurs under tensile loading for ceramic composites tested at room temperature [1-7]. These studies have shown that AE is very effective at determining the onset of damage and to some extent the amount and type of damage (matrix cracking, fiber breaks, etc....). However, due to the modal nature of actual acoustic emission waveforms in thin plates [8-9], the ability to determine the precise location of the sources of the AE signals is very suspect. The dispersive differences in the extensional (symmetric) and flexural (antisymmetric) modes of the waveform as well as the change in the speed of sound due to the reduction in modulus of the composite as damage occurs account for the difficulty in precise source location.

Recently [10], a Modal AE (MAE) approach was taken to quantify the amount of damage, the change in the speed of sound of the extensional mode over the entire stress strain curve, the exact location of the damage, and some physical source identification. The key to the usefulness of this approach for understanding damage accumulation in the composite is the ability to locate events in a section of the composite up to 50 mm from the farthest sensor with good accuracy ($\pm$ 0.5 mm). This is accomplished by determining the difference in times of arrival for the first peaks of the extensional waves at both sensors. This is possible because there is virtually no dispersion of the extensional wave for the frequency range of the first peak (600 to 1000 kHz) and the speed of sound over the entire stress strain curve can be determined.

In this study, the aim is to apply a similar approach to monitor and quantify damage for woven SiC/SiC composites when tested at elevated temperatures. At

---

* Traditional AE , in this paper, refers to the more common use of AE parameters such as counts, amplitude, duration, energy, etc... to characterize AE sources. Resonant frequency transducers are used to detect AE and the waveform is assumed to be a damped sine curve in order to determine the parameters.

intermediate temperatures (600 to 1000°C), the load-bearing capacity of these composites is severely degraded [11-14]. Premature failure in these composites is controlled by oxidation reactions between the environment (O_2 and H_2O) and the interphase (BN for the composite of interest) [13]. The oxidation reactions lead to volatilization of the interphase as well as the formation of condensed phase reaction products (boria liquid and/or borosilicate glass formation). This results in strength degradation of the reinforcing fibers and/or strong bonding between the fibers and the matrix. Both phenomena lead to failure of individual load-bearing fibers at a bridged matrix crack.

Environmental access to the load-bearing fibers is controlled by the extent of matrix cracking. When oxidation occurs in the crack, fibers eventually fail, resulting in a larger stress-intensity at the crack tip which leads to crack growth. This process continues until the applied load on the remaining fibers causes ultimate failure.

The purpose of this study is to report the procedure and discuss the usefulness of MAE in quantifying the location and extent of damage accumulation during high temperature stress-rupture tensile tests. The details of the stress-rupture properties of this material system have been presented elsewhere [15] and will be reported in an upcoming paper.

EXPERIMENTAL

Several properties of the composite constituents are described in Table I. The material consists of eight plies of woven Hi-Nicalon, a ~ 0.5 um boron nitride interphase, and a melt infiltrated (MI) SiC matrix. The matrix was processed in several steps. First a thin (~ 2 μm) layer of SiC was applied to the BN coated woven preform. A SiC particle containing slurry was infiltrated into the porous network. This was followed by infiltration of molten silicon which nearly filled the porous network. Therefore the matrix is predominantly SiC with some Si.

Constituent	Material	Volume Fraction	Elastic Modulus GPa	Details
Fiber	Hi-Nicalon[a]	0.34	280	5 Harness Satin
Interphase	Boron Nitride	0.10	?	~ 0.5 μm thick
Matrix	CVI[b] SiC & MI SiC + Si	0.18 0.38	400	~ 2 mm thickness Process Temp. ~ 1400°C

[a] Nippon Carbon, Tokyo, Japan; [b] Chemical Vapor Deposition Process

The tensile test set-up is shown in Figure 1. Tensile tests were performed using a screw-driven universal testing machine*. The test specimen dimensions were 2.1 mm thickness, 12.5 mm width and 150 mm length. High temperature graphite-epoxy tabs (0.08" thick) were glued to the ends of the bars. The test specimens were gripped with hydraulic grips in the tabbed region. Wide band (50 kHz to 2 MHz) acoustic emission sensors** were attached to the ends of the tensile specimens within the grips with quick setting epoxy. This was done to insure that the temperature the sensors experienced was maintained at approximately 25°C. A resistance-heated furnace ($MoSi_2$ elements) was used to heat the center section of the specimens. The furnace dimension in the tensile direction was 75 mm; however, the hot zone was only approximately 15 mm.

---

* Instron 4502, Instron, Canton, MA

** Digital Wave Corp., Englewood, CO

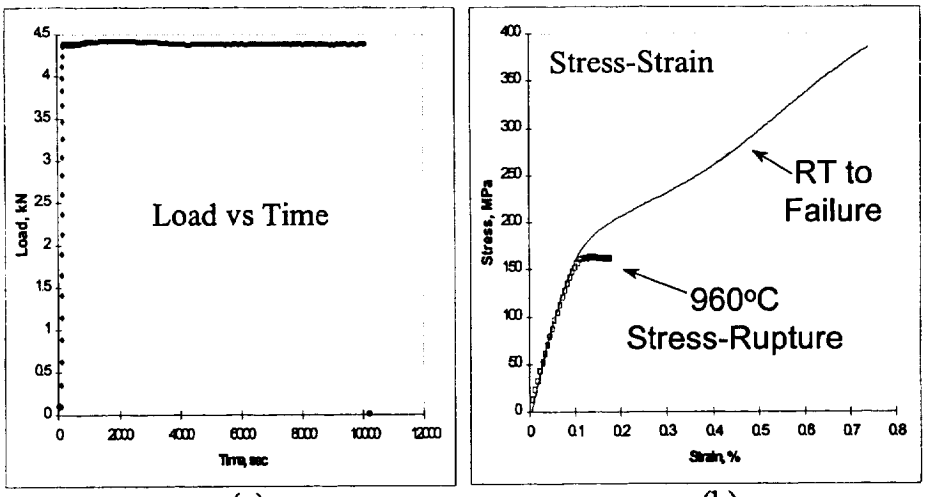

(a) (b)

Figure 2: Load versus time (a) and stress-strain curve of 960°C ruptured specimen. The RT stress-strain curve (b) is from reference 16.

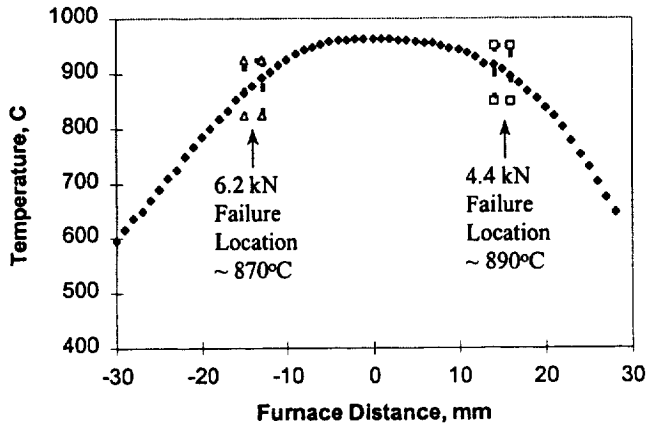

Figure 3: Furnace profile for 960°C and location of composites from two rupture tests.

In order to quantify the damage, all of the events were sorted according to location using a threshold voltage technique (5 mV). The waveforms were then inspected manually in order to correct errors in the location determination due to noise levels greater than 5 mV and/or due to first peaks which had an amplitude lower than 5 mV. Only the events, which were within 30 mm from the center of the hot zone, were accepted. The accepted AE events were further quantified according to the average energy of the two waveforms received on the two sensors for each event.

A typical waveform obtained during the stress-rupture test is shown in figure 4. There are two unique characteristics to this waveform as compared to waveforms obtained during room temperature testing [10,16]. First, the waveform is extensional. This is not surprising since the sensors are attached "ends-on", i.e. not on the face, and the specimen is "clamped" in the grips and the specimen is unable to flex. Second, the waveform is not "symmetrical" about the abscissa after the first peak. This was surprising. It is surmised that this was due to interference of the front of the waveform with the rest of the waveform after the front of the wave reflected back from the edge. All of the waveforms possessed these two characteristics whether they were high or low energy events.

The location of the AE events as a function of time and the applied load as a function of time are shown plotted together in Figure 5a. The location was determined

using a speed of sound 91% of that for the undamaged material based on the change in the speed of sound (difference in times of arrival) for the material subjected to the same applied stress at room temperature [16]. The speed of sound for the undamaged material and the approximated speed of sound used in the location determination were 9600 and 8740 m/sec, respectively. After the test, the speed of sound was determined along the length of the ruptured composite and was found to range from 8570 to 8820 m/sec, confirming the speed of sound approximation.

The load plotted in Figure 5a was from the analog load signal input into the Fracture Wave Detector for each AE event. The apparent load jumps shown in Figure 5a are due to signal noise from the Instron*. Note, in Figure 2a the load output that was conditioned, digitized, and received on a different computer, showed no load fluctuations.

Figure 5b shows the cumulative number of events and cumulative AE energy for the events versus time from the same experiment. Most of the events occur during the stress-rupture portion of the test whereas most of the high energy events occur during initial loading. Therefore, most of the matrix cracks are formed during loading since the high energy events correspond to matrix crack formation [10,16]. Damage continues with time for the stress-rupture condition across the entire 60 mm distance analyzed. Although, AE activity diminishes with time as indicated by the decreasing slope for the number of events vs. time curve (Figure 5b). Virtually no AE activity occurs in the hot zone region after about 5500 seconds (Figure 5a). However, significant AE activity continues just outside of the hot zone region until failure. Two high energy events occurred outside of the hot zone which account for the energy jumps in Figure 5b. One of these events occurred prior to failure and the other was the failure event.

Although high energy AE events occur across the 60 mm of length for the duration of the experiment, it is apparent that a number of high energy events occurred at or near the failure location during the rupture test, i.e. outside the hot zone (Figure 5a). These high energy events near the failure location must correspond to the phenomena described above (Introduction) where fiber degradation and reaction product formation lead to matrix crack growth and ultimate failure of the composites under these conditions.

Figure 5a shows the location of the composite failure as measured from the two ends of the specimen. The fracture surface was "jagged" and spanned a distance of ~ 2 mm in the loading direction. The final AE event (highest energy event) which corresponded to failure was determined to be less than 2 mm from the measured location. This was considered an excellent correlation. The location of the failure events for all five of the stress-rupture tests determined from the difference in times of arrival were always within 1 or 2 mm of the measured location.

To correlate the observed AE behavior with damage accumulation along the length of the specimen, a portion of the failed test specimen which included the hot zone exposed region was cut into segments, polished longitudinally, and plasma etched with HF in order to enhance the cracks. This was performed for the two failed specimens tested at 960°C (Figure 3). The number of cracks was determined for an internal ply and a surface ply along the length. There was never more than a 10% difference for the number of cracks in the two plies. The two values were averaged and the average crack spacing was determined over the measured distance. The data are shown in figure 6 along with the temperature profile for both samples. It is apparent that more cracking occurred in the 700 to 900°C regime for both samples compared to the amount of

---

* This was determined by connecting an oscilloscope to the output from the Instron. A periodic, low frequency noise always occurred even when no load was applied. This noise had no effect on the AE signals.

cyclic fatigue test at temperature. This would allow in-situ monitoring of the damage mechanisms causing failure at elevated temperature and the location of the potential failure site.

CONCLUSION

Modal AE was used to successfully monitor and locate damage accumulation in a SiC fiber reinforced SiC matrix composite during elevated tensile stress-rupture tests in air. Wide band transducers had to be mounted on the edge of the specimens in the cold, grips of the test frame in order to shield the sensors from high temperature exposure. The composite failure location was determined to within 1 or 2 mm of the actual failure location. Increased AE activity was observed outside of the furnace hot zone, i.e. at lower temperatures than the hot zone. The amount of AE activity, which was based on the energy of the waveforms, corresponded well with the measured matrix cracking over the length of the composite that was exposed to a wide temperature range. Therefore, modal AE was effective at monitoring the location and extent of damage as a function of the stress-strain condition, time, and temperature (spatial location).

ACKNOWLEDGMENTS

The BN infiltration and CVI SiC infiltration were performed by DuPont Lanxide Composites Inc., Newark, DE. The MI SiC infiltration was performed by Carborundum Corporation, Niagra Falls, NY. Special thanks to Janet Hurst of NASA Lewis Research Center and Dan Gorican of Gilcrest for use of their equipment and expertise in performing the rupture tests. Thanks also to Dr. Andrew Gyekenyesi for review of the manuscript. This work was supported by the HITEMP program at NASA Lewis Research Center.

REFERENCES:

1. R.Y. Kim and N.J. Pagano, J. Am. Ceram. Soc., 74, 1082 (1991)
2. O. Chen, P. Karandikar, N. Takeda, T. Kishi, W. Tredway, and K. Prewo, Ceram. Eng. Sci. Proc., 12, 1586 (1991)
3. A. Chulya and J.P. Gyekenyesi, presented at International Gas Turbine and Aeroengine Congress and Exposition, The Hague, Netherlands – June 13-16, 1994, AMSE publication 94-GT-444
4. J.J. Luo, S.C. Wooh, and I.M. Daniel, J. Comp. Materials, 29, 1946 (1995)
5. G.N. Morscher and J. Martinez-Fernandez, J. Am. Ceram. Soc., 79, 1083 (1996)
6. M. Surgeon, E. Vanswijgenhoven, M. Wevers, and O. Van Der Biest, Composites Part A, 28A, 473 (1997)
7. N. Lissart and J. Lamon, Acta mater., 45, 1025 (1997)
8. M.R. Gorman, J. Acoust. Soc. Am., 90, 358 (1991)
9. M.R. Gorman, AMD-Vol. 188, Wave Propagation and Emerging Technologies, ASME, 47 (1994)
10. G.N. Morscher, Comp. Sci. Tech., in print
11. F.E. Heredia, J.C. McNulty, F.W. Zok, and A.G. Evans, J. Am. Ceram. Soc., 78, 2097 (1995).
12. H.T. Lin and P.F. Becher, Composites Part A, 28A, 935 (1997)
13. G.N. Morscher, J. Am. Ceram. Soc., 80, 2029 (1997)
14. E. Lara-Curzio, J. Am. Ceram. Soc., 80, 3268 (1997)
15. G.N. Morscher, presented at the annual American Ceramic Society Conference, Cincinnati, OH. May 4th, 1998
16. G.N. Morscher and J.Z. Gyekenesi, Ceram. Eng. Sci. Proc., 1998
17. N.S. Jacobson and G.N. Morscher, J. Am. Ceram. Soc., in print.